SUPPLEMENTAL MATERIAL

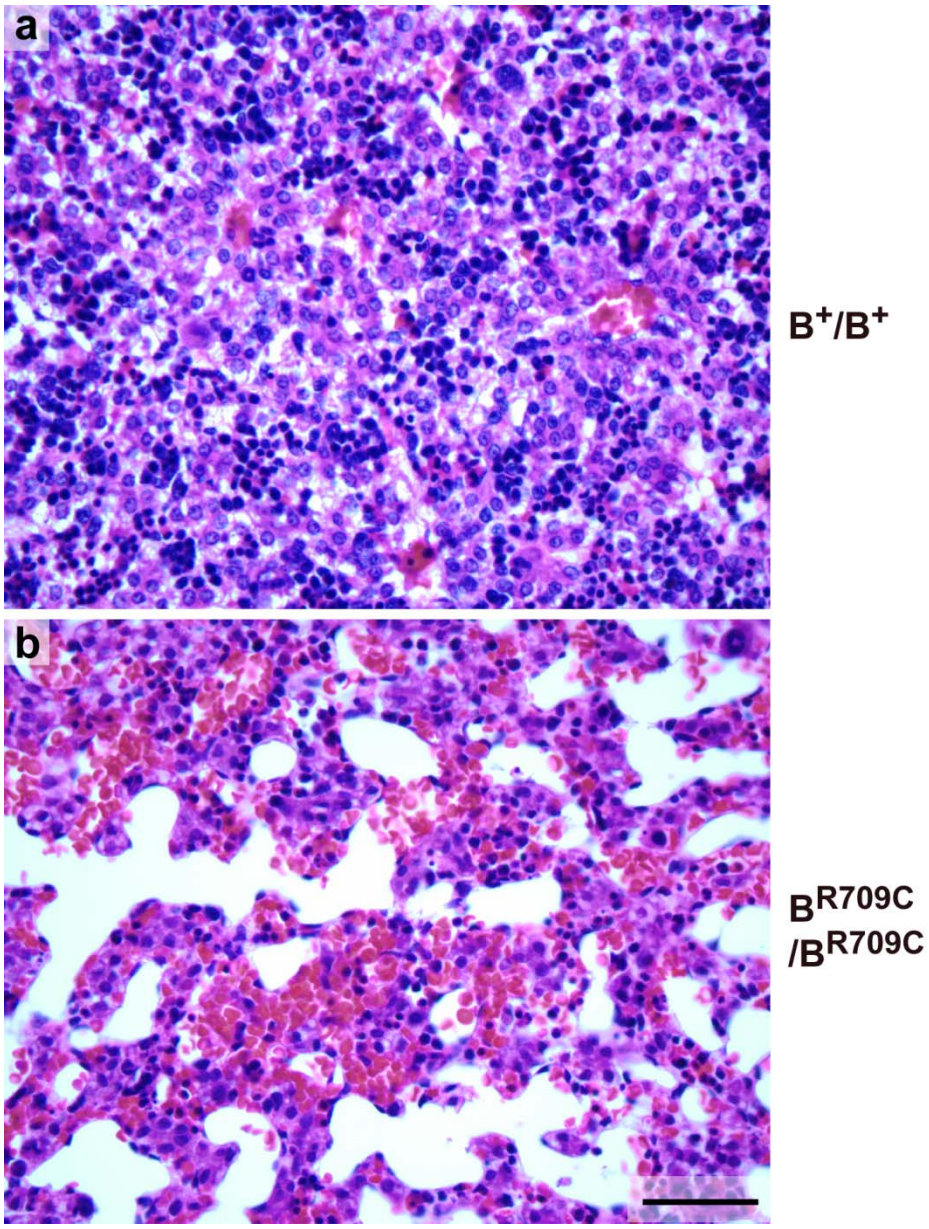

Figure S1. Congested B^{R709C}/B^{R709C} Mouse Liver. a,b. H&E stained sections of E14.5 mouse liver from B^{+}/B^{+} (a) and B^{R709C}/B^{R709C} (b) mice show sinusoidal dilation and accumulation of blood cells in the B^{R709C}/B^{R709C} liver. Scale bar: 200 μm.

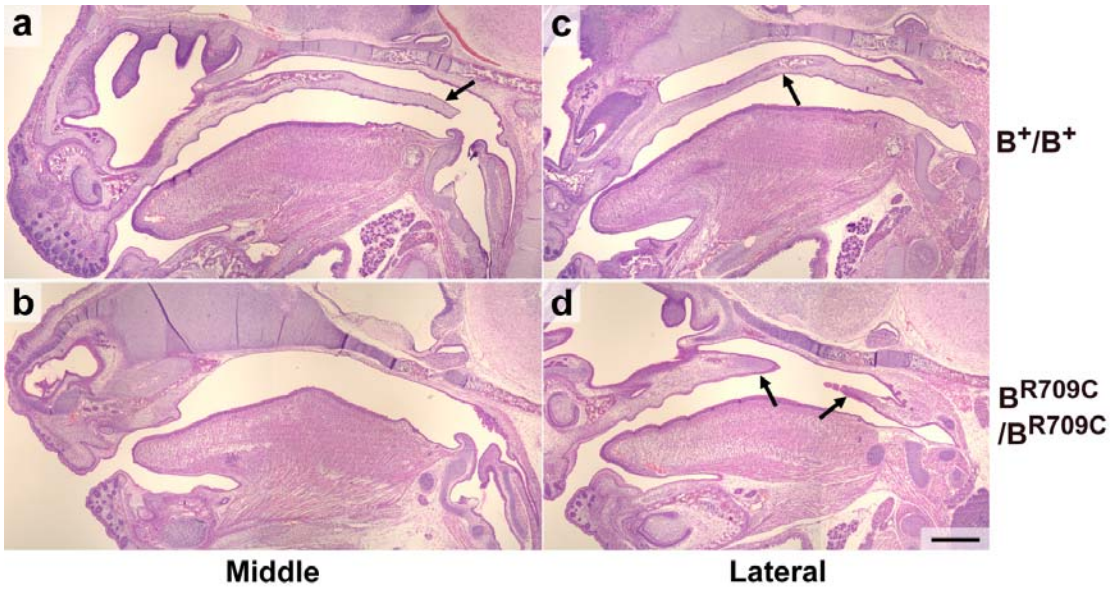

Figure S2. Cleft Palate in E16.5 B^{R709C}/B^{R709C} Mice. a-d. H&E stained sagittal sections of E16.5 embryos show a cleft palate in B^{R709C}/B^{R709C} mice. Panels a and b are sections through the middle of the mouse heads, and panels c and d show lateral sections. The palate is completely missing at the middle section (b), and shows a large gap at a lateral section (d) in B^{R709C}/B^{R709C} mice. Normal B^{+}/B^{+} sections are shown in panels a and c. Arrows in panels point to the palatal shelves. Scale bar: 200 μm.

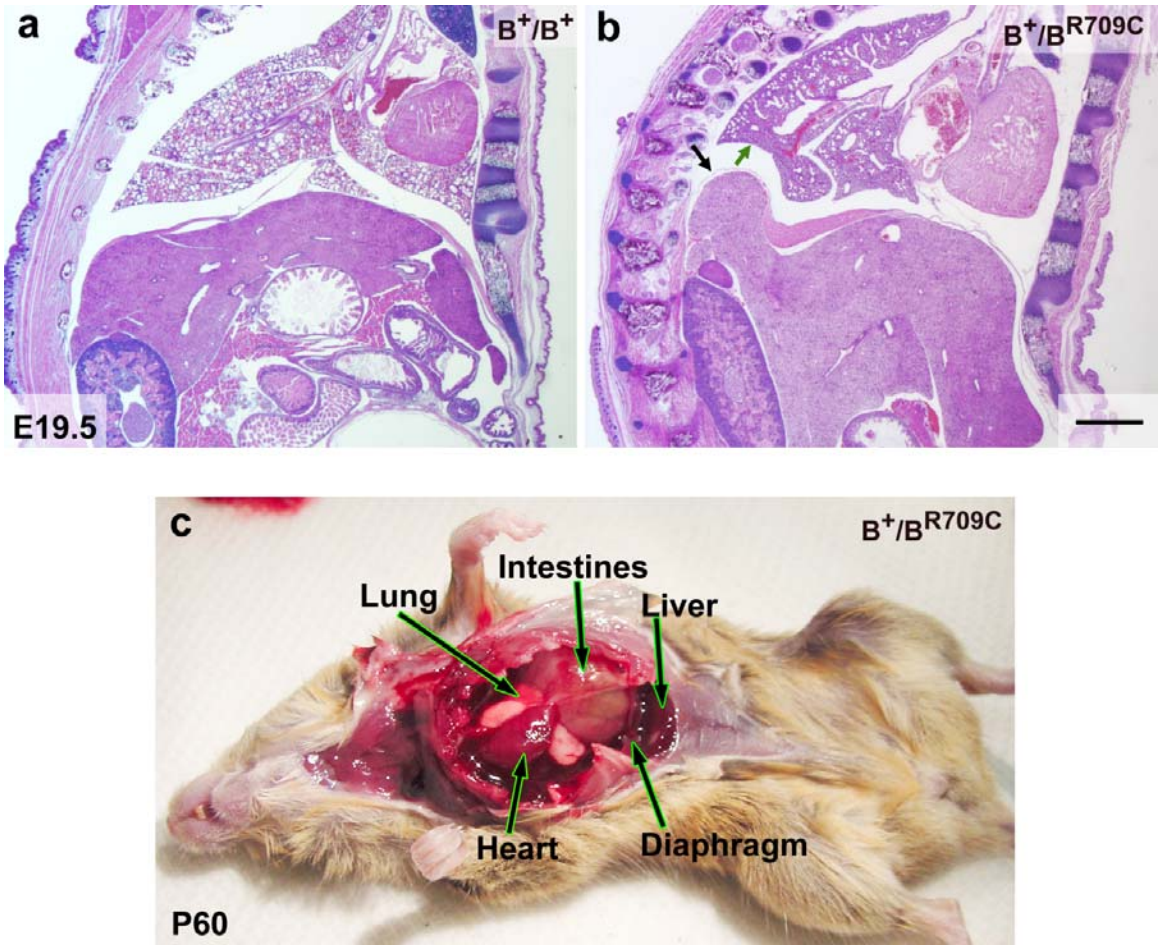

Figure S3. Diaphragmatic Hernia in B^{+}/B^{R709C} Mice. a,b. H&E stained sagittal sections of E19.5 embryos show a diaphragmatic hernia in B^{+}/B^{R709C} mice where the liver is protruding into the thoracic chamber (b, black arrow). The invasion of the liver into the thorax has pressed against the developing lung (b, green arrow) and shifted its location . A B^{+}/B^{+} embryo shows the normal position of the liver and lung (a). Panel c shows an adult (P60) B^{+}/B^{R709C} mouse with most of its intestines herniated into the thoracic chamber (c). The abdominal cavity only contained the liver and rectum (not opened). Scale bar: panels a and b, 1 mm.

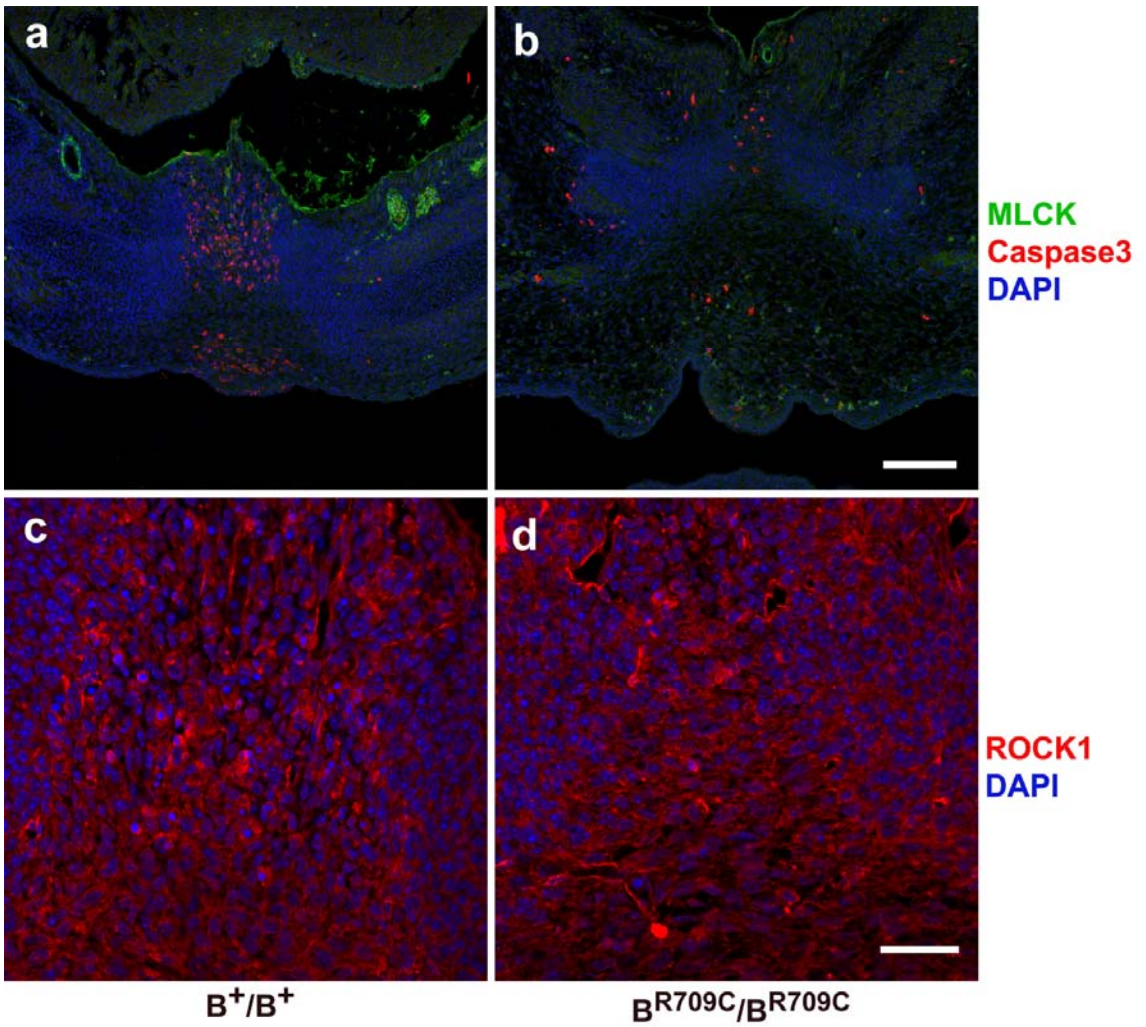

Figure S4. Expression of MLCK and ROCK1 in the Fusing Sternal Area. a,b. Confocal images of the sternal area stained with antibodies for MLCK (green) and activated-caspase-3 (red) from E14.5 mouse embryos show no obvious expression of MLCK in fusing sternal area (a) which contains a large number of activated caspase-3 positive mesenchymal cells in B^{+}/B^{+} mice (a, red). MLCK is also not detected in B^{R709C}/B^{R709C} sternum (b) which shows a reduced number of activated caspase-3 positive mesenchymal cells. MLCK is detected in methothelial cells and vessels (a,b, green). c,d. Confocal images of E14.5 mouse embryos stained with antibodies for ROCK1 (red) show that ROCK1 is expressed in the fusing sternum of B^{+}/B^{+} and B^{R709C}/B^{R709C} mice. Nuclei are stained with DAPI (blue). Scale bars: panels a and b, 200 μm; c and d, 50 μm.

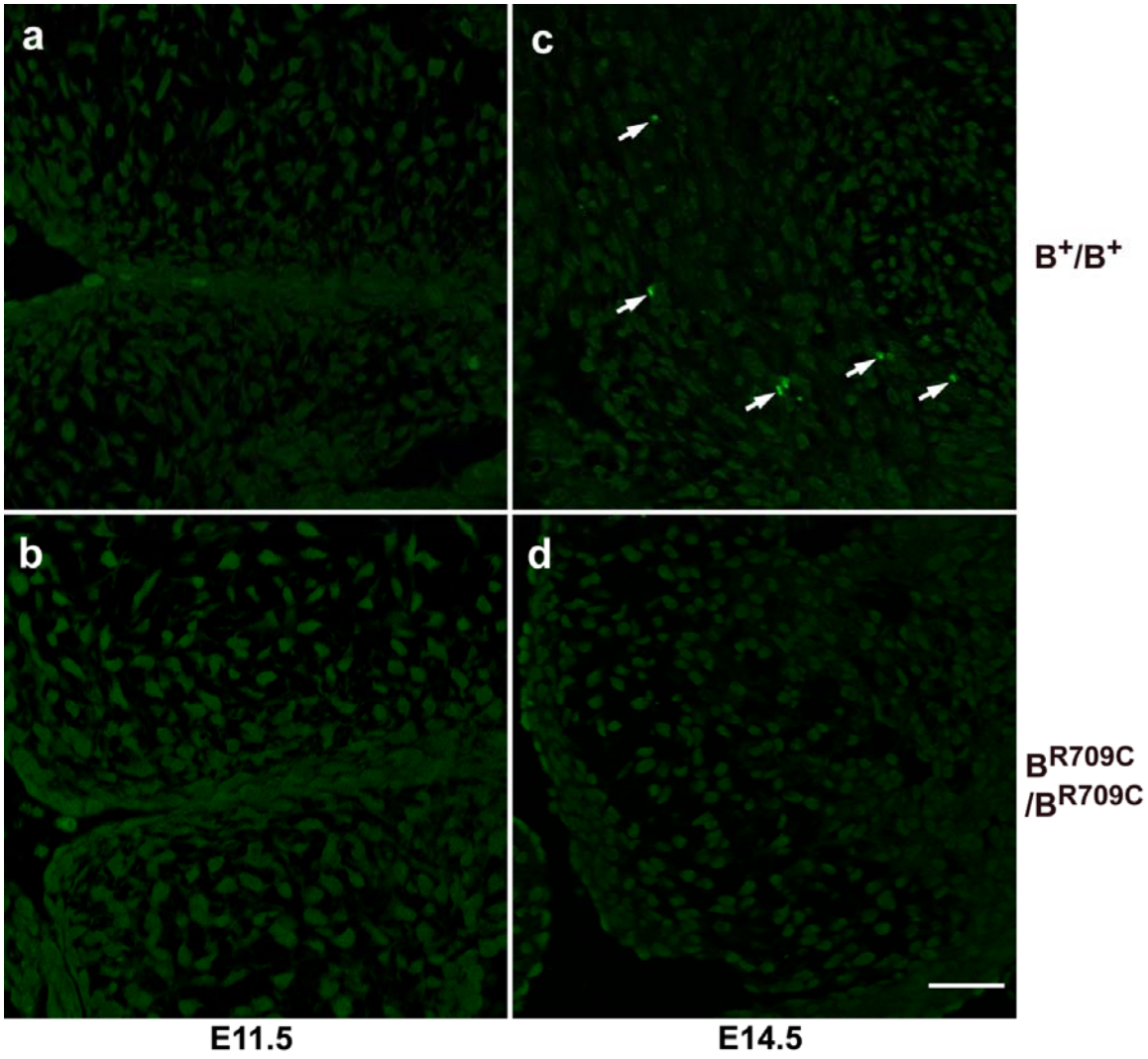

Figure S5. Impaired Apoptosis in B^{R709C}/B^{R709C} AV Cushions. a-d. TUNEL assay shows apoptotic cells in developing atrioventricular cushions from E11.5 and E14.5 B^{+}/B^{+} (a,c) and B^{R709C}/B^{R709C} (b,d) mice. Both B^{+}/B^{+} (a) and B^{R709C}/B^{R709C} (b) cushions show no apoptotic cells at E11.5. At E 14.5 apoptotic cells were observed in B^{+}/B^{+} cushions (c, arrows), but not found in B^{R709C}/B^{R709C} cushions (d). Scale bar: 50 μm.

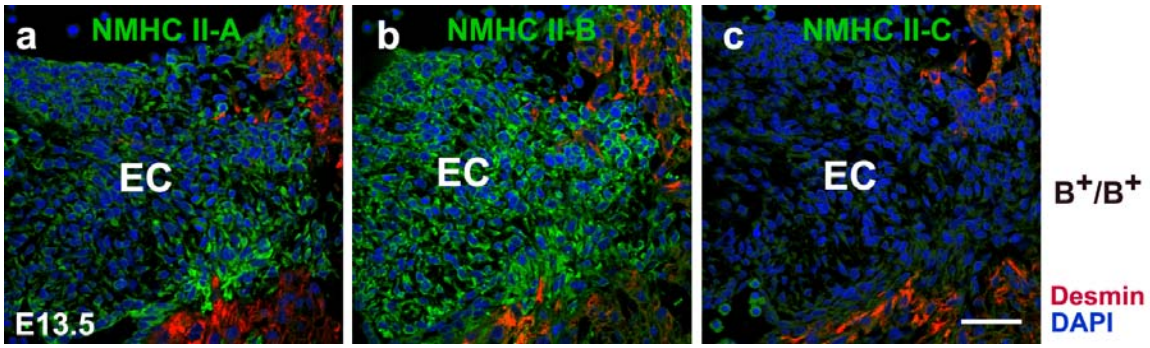

Figure S6. Expression of NMHCII-A, II-B and II-C in the Developing Mouse AV Cushions. a-c. Immunofluorescence confocal microscope images of E13.5 B^+/B^+ AV cushions stained with antibodies for NMHCII-A (a), II-B (b) and II-C (c) show that NMII-A and II-B, but not II-C, are expressed in the developing AV cushions. Desmin (red) stains the cardiac myocytes. Scale bar: 40 μm.

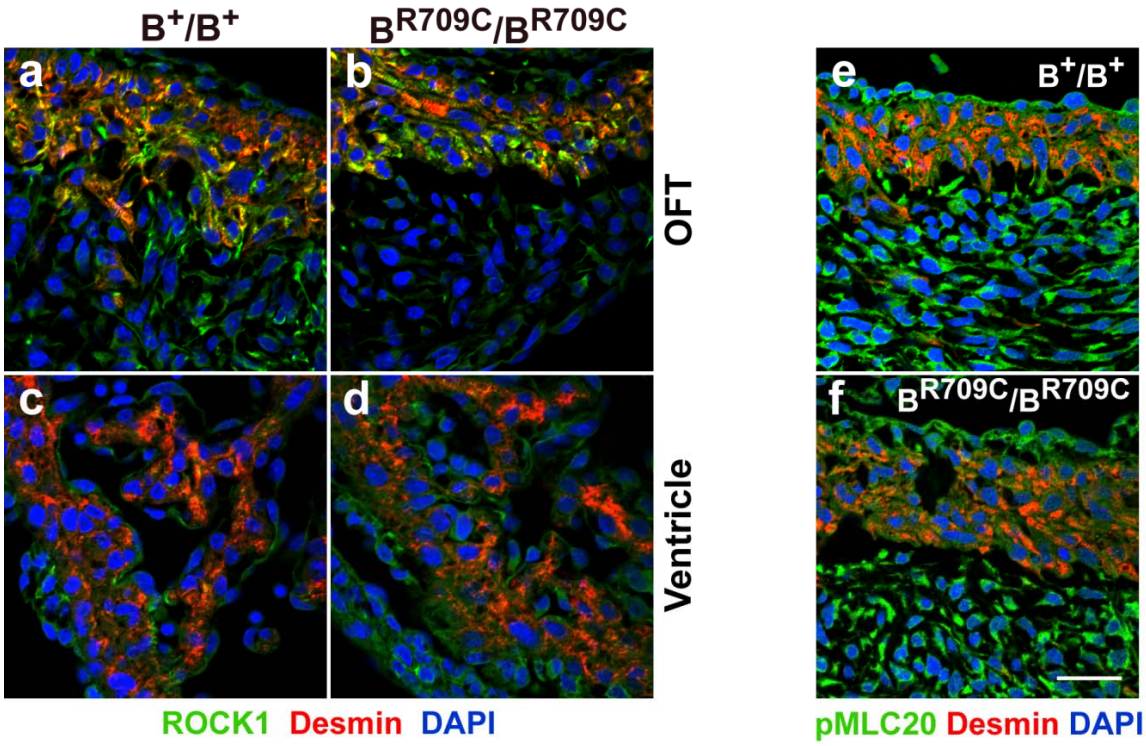

Figure S7. ROCK1 Expression and NMII-B Phosphorylation in B^{+}/B^{+} and B^{R709C}/B^{R709C} Mouse Hearts. a-d. Immunofluorescence confocal microscope images of E11.5 mouse hearts stained with antibodies for ROCK1 (green) and desmin (red, marker for myocytes) show that ROCK1 is predominantly expressed in OFT cardiac myocytes in both B^{+}/B^{+} (a, green) and B^{R709C}/B^{R709C} (b, green) mouse hearts, but not in ventricular myocytes (c,d). ROCK1 stains cardiac non-myocytes in ventricles (c,d, green). MLCK is detected in myocytes in the OFT and in the ventricle (see Figure S7). e,f. Phospho-MLC20 (pMLC20) is detected in OFT cardiac myocytes in both B^{+}/B^{+} (e, green) and B^{R709C}/B^{R709C} (f, green) mouse hearts. The cardiac myocytes were stained with desmin antibody (red). DAPI (blue) stains nuclei. Scale bar: 40 μm.

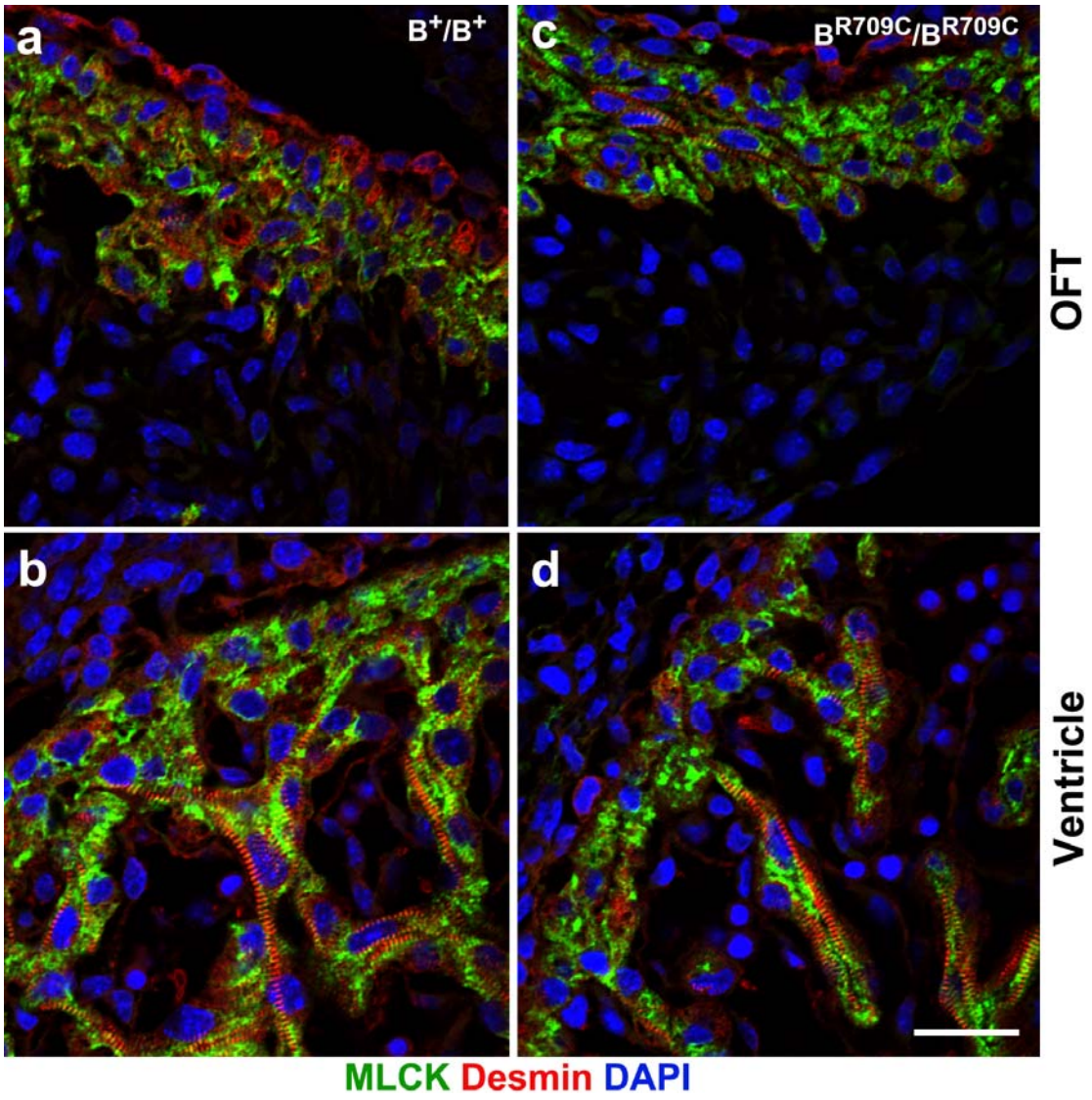

Figure S8. MLCK Expression in Developing Outflow Tract and Ventricular Cardiac Myocytes of B^{+}/B^{+} and B^{R709C}/B^{R709C} Mouse Hearts. a-d. Immunofluorescence confocal microscope images of E11.5 mouse hearts stained with antibodies for MLCK (green) and desmin (red, marker for myocytes) show that MLCK is detected in both OFT and ventricular myocytes from B^{+}/B^{+} (a,b) and B^{R709C}/B^{R709C} (c,d) mice. Nuclei are stained with DAPI (blue). Scale bar: 40 μm.

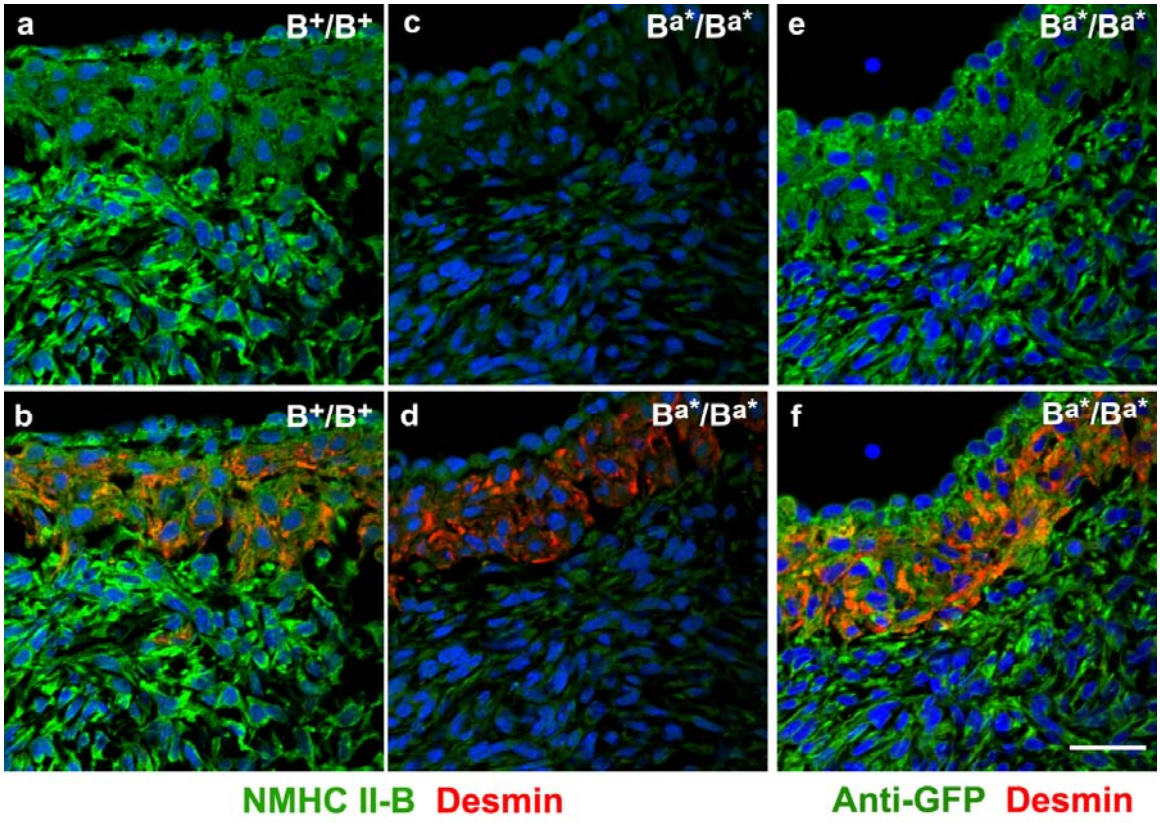

Figure S9. Expressing Nonmuscle Myosin II-A in Place of Nonmuscle II-B (B^{a*}/B^{a*} Mice) Does not Rescue Myocardialization Defects in the Developing Outflow Tract

a-f. Immunofluorescence confocal microscope images of the OFT from E11.5 mouse hearts stained with antibodies for NMHCII-B (a-d, green), GFP (e,f, green, staining for EGFP-tagged NMHCII-A) and desmin (red, marker for cardiac myocytes) show that NMHCII-B is expressed in B^{+}/B^{+} cardiac myocytes (a, green), but not in B^{a*}/B^{a*} cells (c). Expression of EGFP-NMHCII-A in place of NMHCII-B is confirmed by positive staining for GFP in B^{a*}/B^{a*} mouse heart (e, green). The cardiac myocytes (red) are invading the underlying cardiac cushions in the B^{+}/B^{+} mouse heart (b) but not in the B^{a*}/B^{a*} heart (d,f). Nuclei are stained with DAPI (blue). Scale bar: 40 μm.

Table S1. List of Primary Antibodies Used in Immunostaining

Antibodies	Source and Working Condition
NMHC II-A	1:1000, Covance, Emeryville, CA
NMHC II-B	1:3000, Covance, Emeryville, CA
NMHC II-C	1:1000, Covance, Emeryville, CA
N-cadherin	1:200, Zymed, South San Francisco, CA
Cleaved Caspase-3	1:200, Cell Signaling Technology, Inc., Danvers, MA
Desmin	1:100, DakoCytomation, Denmark
MF20	1:30, Developmental Studies Hybridoma Bank, University of Iowa, IA
ROCK1	1:100, Abcam, Cambridge, MA
Phosph-MLC20	1:100, Cell Signaling Technology, Inc., Danvers, MA
MLCK	1:2000, Sigma, St. Louis, MO
P53	1:100, Abcam, Cambridge, MA

Table S2. Echocardiography (E14.5)

	HR	LVDd (cm)	LVDs (cm)	FS (%)
B^{+}/B^{+} (n=4)	180	0.086	0.036	58
B^{R709C}/B^{R709C} (n=3)	116	0.090	0.080	11

HR: heart Rate; LVDd: left ventricle dimension in diastole;
LVDs: left ventricle dimension in systole; FS: fractional shortening